J Mater Sci: Mater Med (2008) 19:2637–2645
DOI 10.1007/s10856-007-3362-5

# Fabrication of bioactive hydroxyapatite/bis-GMA based composite via three dimensional printing

**J. Suwanprateeb · R. Sanngam · W. Suwanpreuk**

Received: 22 October 2007 / Accepted: 28 December 2007 / Published online: 16 January 2008


**Abstract** Hydroxyapatite/bis-GMA composites were processed by new technique which comprised three dimensional printing (3DP) of hydroxyapatite and then impregnation by bis-GMA based resin. Two types of composites which used either as-fabricated green 3DP samples or 1,300°C sintered 3DP samples were studied. It was found that both 3DP composites have higher flexural modulus, strength and strain at break than the initial 3DP hydroxyapatite sample. Composites produced from sintered sample has higher hydroxyapatite content, higher density and greater modulus, but lower strength and strain at break than composite produced from green 3DP sample. In vitro toxicity shows that 3DP hydroxyapatite/bis-GMA based composites are non-toxic. Osteoblast cells were observed to attach and attain normal morphology on the surface of composites.

## 1 Introduction

Synthetic hydroxyapatite has a chemical formulation resembling the main inorganic mineral constituent in bone. Using a synthetic compound that is similar to bone apatite is perceived to be advantageous for replacing the hard tissue. Therefore, it has been used as bone replacement materials for the last 20 years. It possesses excellent biocompatibility and is osteoconductive. It has been used clinically on its own as a bioactive material in the form of powder, porous structure, or dense body. However, although it is hard and strong material, the brittleness is the weak properties. Many attempts to increase the toughness hydroxyapatite have been researched. One of the famous routes is to use hydroxyapatite as fillers for other materials. Previous studies have shown that by blending hydroxyapatite and polymers, bioactive composites have been produced which have greater toughness than hydroxyapatite alone, but still retain biocompatibility and bone-bonding ability [1–13].

From an implant manufacturing point of view, traditional techniques which have been used to prepare such composites are by mixing components together and specimens are then fabricated by moulding for example compression moulding, injection moulding or casting. Although these techniques could be used to fabricate an implant by casting or hand sculpting, the aesthetic and fitting are sometimes compromised. In addition, it is time-consuming and if the shape of defect is highly complicated, the manual fabrication is impossible. Solid freeform fabrication (SFF) or rapid prototyping (RP) is a computerized fabrication technology that additively builds highly complex 3D physical objects layer by layer using data generated by computer, for example CAD or digital graphic [14–16]. This technology is very useful in medical applications to fabricate a 3D physical object from digital data of patients acquired from a medical imaging system such as CT or MRI. The replica models can be then used for visualization and modeling tools to aid with pre- or per-operative planning and production of patient medical models or customized implants [17–24]. Three dimensional printing (3DP) is one of such technologies which employs ink jet printing technology for processing powder materials. During fabrication, a printer head is used to print a liquid onto thin layers of powder following the object's

J. Suwanprateeb (✉) · R. Sanngam · W. Suwanpreuk
National Metal and Materials Technology Center, National Science and Technology Development Agency, Ministry of Science and Technology, 114 Paholyothin Road, Klong 1, Klongluang, Pathumthani 12120, Thailand
e-mail: jintamai@mtec.or.th

profile as generated by the system computer. Subsequently, a cylinder containing the powder bed is lowered, allowing for the spread of the next powder layer. Unbound powder temporarily supports unconnected portions of the component, allowing overhang, undercut and internal volumes to be formed. The unbound powder is vacuumed or brushed away upon process completion, leaving the finished green part. The advantage of this technology is that it can fabricate a highly complex structure readily.

Previously, hydroxyapatite sample was successfully produced by this 3DP technique, Fig. 1, but low mechanical properties and brittleness were observed [25]. It is speculated that by combining with polymers to produce composites would increase the mechanical properties. In this study, 3DP in couple with resin impregnation technique is investigated as an alternative tool to fabricate bioactive composites based on Bis-GMA and hydroxyapatite for bone substitution. Bis-GMA based resin is selected as a matrix in composites since it is a low volatile liquid which can penetrate through 3DP sample easily and transform into strong solid upon polymerization reaction by various means. This is suitable for resin impregnation technique that would be used in this study. In addition, it has been shown previously that this resin could be mixed

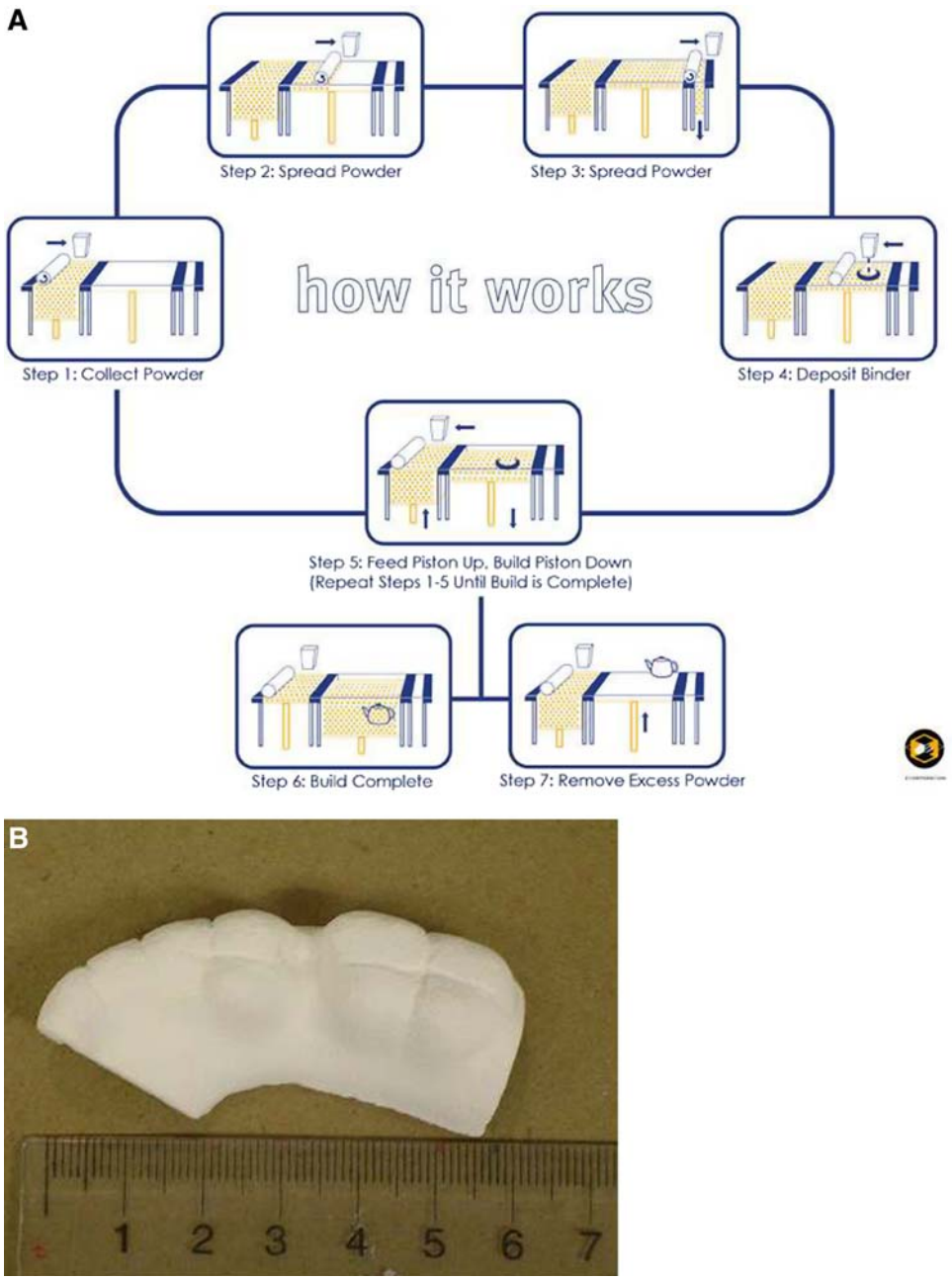


**Fig. 1** Three dimensional printing process and tooth model of hydroxyapatite as fabricated by 3DP process

with hydroxyapatite to form bioactive composites with good mechanical and biological properties targeting as a new bone cement, dental restoration materials and bone replacement materials [10–13]. Physical and mechanical properties and in vitro cell toxicity of developed composites were reported in this study.

## 2 Materials and methods

### 2.1 Materials

Raw materials used in this study were hydroxyapatite (Taihei Chemical Industrial, Japan) with an average particle size of 3–5 μm and maltodextrin (Shandong Duqing, Inc., China) with an average particle size of 90–100 μm. Impregnation material used was clear heat-cured acrylate resin prepared by mixing triethylene glycol dimethacrylate (TEGDMA), 2,2-bis[4 (2-hydroxy-3-ethacryloyloxypropyloxy)-phenyl]propane (bis-GMA) and urethane dimethacrylate (UDMA) which were procured from Esschem, USA, at the proportion of 40:40:20 wt.% in a beaker. The mixture was stirred for 1 h and 1% of iniator, benzoyl peroxide, was then added.

### 2.2 Specimen preparation

Slurry of hydroxyapatite mixture was prepared by mixing as-received hydroxyapatite powder with maltodextrin at the weight ratio of 2:1 in water. Darvan C (R.T. Vanderbilt Company, Inc., USA) was used as a dispersing agent in all formulations. The slurry mixture was ball-milled overnight. It was then spray dried using a spray dryer (Niro A/S, Denmark) to achieve pre-coated hydroxyapatite powders which had an average particle size of 80 μm and were used as raw materials for specimen fabrication by a 3DP machine (Z400, Z Corporation, USA). Green specimens ($80 \times 10 \times 4$ mm$^3$) were printed using a layer thickness of 0.175 mm (designated HA-g). Water-based binder was used as a jetting media in all formulations. After building, all the specimens were left in the machine for 2 h before taken out and left for drying outside for 24 h. The specimens were then air blown to remove the unbound powders. In the case of sintered specimens (designated HA-s), the green specimens (HA-g) were sintered at 1,300°C for 3 h in normal air atmosphere. The HA-g and HA-s specimens were then immersed in liquid bis-GMA/TEGDMA/UDMA mixture in vacuum condition at 1000 mbar (MCP vacuum casting machine model 4/01) for 5 min. The impregnated composite specimens were then taken out from the beaker, blotted by a tissue paper to eliminate an excess liquid on the surface and cured by placing the specimens in an air-circulated oven at 105°C for 180 min and then post cured at 120°C for 30 min. These composites were designated as HA-bisGMA-g and HA-bisGMA-s, respectively. The bis-GMA/TEGDMA/UDMA resin was also casted in silicone mould for using as controlled specimen for comparison.

### 2.3 Thermogravimetric analysis

Measurement of hydroxyapatite content in the composites was performed by a thermogravimetric analyzer (Metler-Toledo TGA System). Small pieces of the composites were cut from the specimens and then scanned in the instrument at temperatures ranging from room temperature to 600°C at the rate of 20°C/min. Changes in weight of the samples were monitored and then analyzed by the TGA analysis program.

### 2.4 Microstructure and fractography examination

Microstructure of raw material and fracture surface of specimens were examined using a scanning electron microscope (JSM-5410, JEOL, Japan) at the accelerating voltage of 20 kV. All samples were gold sputtered prior to the observation.

### 2.5 Bulk density determination

Bulk density was determined by measuring all dimensions of the specimen by a vernier caliper (Mitutoyo) with the reading resolution of 0.01 mm. The measurement was done three times in each direction and the values were then averaged. Volume was calculated by multiplying width, thickness and length. The weight of specimens were measured by a digital balance (Mettler Toledo PB4002-S) with the reading resolution of 0.001 g. Density was then calculated by dividing the weight by the volume.

### 2.6 Flexural testing

Flexural tests were performed on a universal testing machine (Model 55R4502, Instron Corporation, USA) equipped with a 10 kN load cell. All the tests were carried out according to ASTM D790 at 23°C and 50% RH using three point bending method and a constant crosshead speed of 0.5 mm min$^{-1}$. The HA-g and HA-bisGMA-g specimens were in the form of rectangular bar with dimensions of $80 \times 10 \times 4$ mm$^3$ whereas the dimensions of HA-s and HA-bisGMA-s specimens were lower due to the shrinkage ($\sim$20%) after sintering ($64 \times 8 \times 3.2$ mm$^3$). However, the span length was equally set as 64 mm for all samples.

### 2.7 In vitro cell toxicity

Composite samples were tested for toxicity by direct contact method using human osteoblast cells (h-OBs). The SFJm medium was supplemented with foetal bovine serum and antibiotics. All the samples were autoclaved at 121°C for 15 min prior to cell culture studies. Ten thousand cells per 1 ml of media were added to each tissue culture dish containing samples, or to an empty tissue culture dish as a reagent control. Thermanox and Portex Control PVC were used as negative and positive control respectively. The incubation period was 6 days. After 6 days, the morphology of cells was then observed using inverted light microscope after staining the cells with neutral red to observe to cell viability. In the case of cell characteristic on the surface of samples, the cultured samples were dried using a critical point dryer, gold sputtered and then observed by scanning electron microscope (JSM-6301F, JEOL, Japan) at the accelerating voltage of 3 kV.

## 3 Results

Figure 2 shows the original morphology of as-received hydroxyapatite powder used in this study. It can be seen that it comprises agglomerates of needle-like crystals. After pre-coating by spray drying process, the morphology of hydroxyapatite particles change to spherical shape consisting of multiple hydroxyapatite particles which were coated and binded by maltodextrin. Table 1 shows the weight fractions of hydroxyapatite in hydroxyapatite/bis-GMA based composites which were determined by TGA analysis. The contents of hydroxyapatite are found to be 0.41 and 0.57% for HA-bisGMA-g and HA-bisGMA-s, respectively. When these weight fractions are converted to volume fraction, the calculated volume fractions are 0.22 and 0.36 for HA-bisGMA-g and HA-bisGMA-s, respectively. Table 2 shows the bulk densities of composites in comparison to 3DP hydroxyapatite and bis-GMA based resin which was used as a matrix in composite. It can be seen that both types of composites have higher bulk densities than 3DP hydroxyapatite and matrix resin. In addition, density of HA-bisGMA-s is greater than density of HA-bisGMA-g composite.

Figures 3–5 show the comparison of flexural properties of studied materials. All composites have significantly greater flexural modulus, strength and strain at break than their as-fabricated 3DP hydroxyapatite counterpart. In comparison to the matrix resin, bis-GMA based resin has greater strength and strain at break than composites. However, flexural modulus of bis-GMA based resin is lower than of composites. HA-bisGMA-g show slightly lower flexural modulus than HA-bisGMA-s. However,

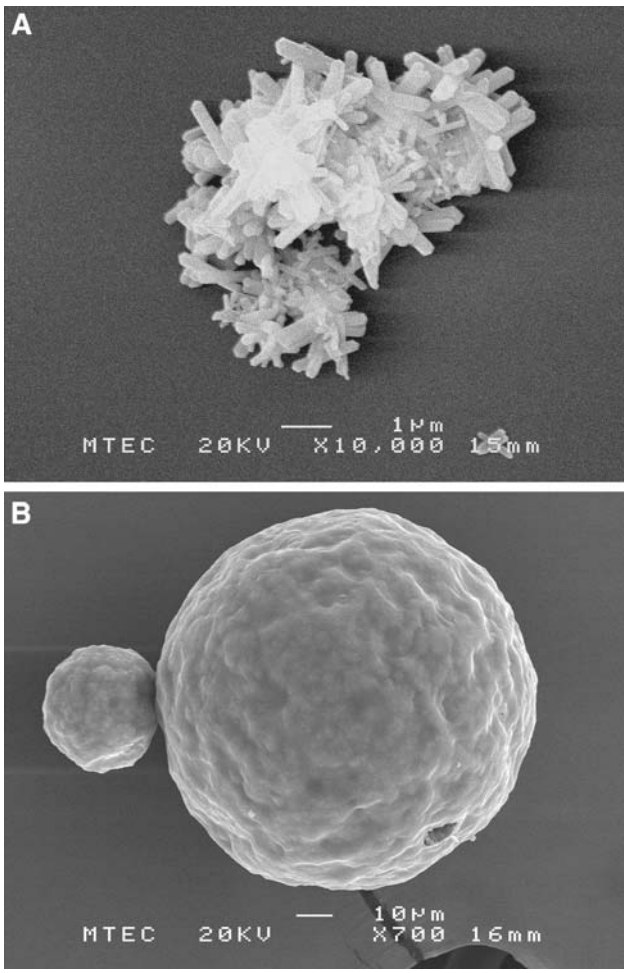


**Fig. 2** SEM micrograph of as-received and spray-dried hydroxyapatite particles

**Table 1** Weight and volume fraction of hydroxyapatite in composites as determined by thermogravimetry

| Formulations | TGA derived weight fraction of hydroxyapatite (w/w) | Calculated volume fraction of hydroxyapatite (v/v) |
|---|---|---|
| HA-bisGMA-g | 0.41 | 0.22 |
| HA-bisGMA-s | 0.57 | 0.36 |

**Table 2** Bulk densities of 3DP fabricated materials

| Materials | Bulk density (kg $m^{-3}$) | Calculated density based on rule of mixture (kg $m^{-3}$) |
|---|---|---|
| HA-g | 806 ± 10 | N.A. |
| HA-s | 964 ± 20 | N.A. |
| HA-bisGMA-g | 1,540 ± 110 | 1,583 |
| HA-bisGMA-s | 1,730 ± 40 | 1,867 |
| bis-GMA/TEGDMA/UDMA | 1,138 ± 30 | N.A. |

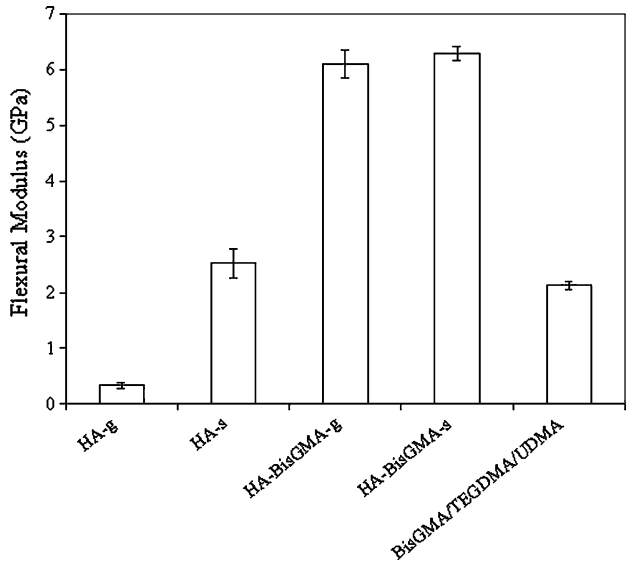


**Fig. 3** A comparison of flexural modulus of 3DP composites, 3DP hydroxyapatite and matrix resin

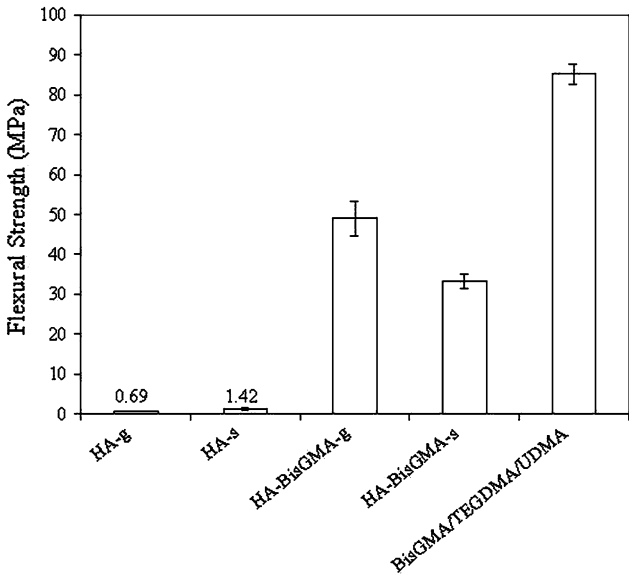


**Fig. 4** A comparison of flexural strength of 3DP composites, 3DP hydroxyapatite and matrix resin

flexural strength and strain at break of HA-bisGMA-g are greater than HA-bisGMA-s composite.

Figures 6a and 7a show general fracture surface of 3DP fabricated composites. Both composites are similar in that the hydroxyapatite particles were distributed in the bis-GMA continuous matrix. However, the content of resin matrix in HA-bisGMA-g was clearly greater than in HA-bisGMA-s. It could also be seen that fracture surface of HA-bisGMA-g was flat while the fracture surface of HA-bisGMA-s was rough. The complete debonding of hydroxyapatite particles was

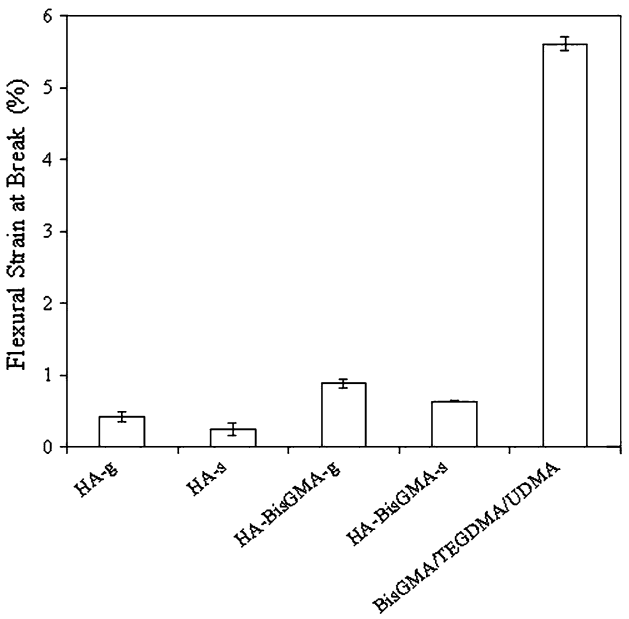


**Fig. 5** A comparison of flexural strain at break of 3DP composites, 3DP hydroxyapatite and matrix resin

observed in both composites without residual resin on the surface of hydroxyapatite particles indicating low interfacial strength, Figs. 6b and 7b. Upon close examination on hydroxyapatite particles in the composites as shown in Figs. 6c and 7c, hydroxyapatite particles in HA-bisGMA-g composite was agglomerate consisting of multiple hydroxyapatite crystals which were coated and binded by maltodextrin through dissolution and solidification process whereas hydroxyapatite particles in HA-bisGMA-s consisted of crystals which were melted and binded together by heat.

In vitro cell toxicity shows that both HA-bisGMA-g and HA-bisGMA-s are non-toxic to osteoblast cells as the cells were neutral red stained indicating vital cells. Figures 8a and 9a show the scanning electron microscope pictures of osteoblast cells cultured for 6 days on HA-bisGMA-g and HA-bisGMA-s composites. The live cells appear to adhere and attain a normal morphology on surfaces of both composites. Osteoblast cells were observed to spread well and attach to the specimen surface. Figures 8b and 9b depict higher magnification of single osteoblast cell showing the extension of cell to attach itself to hydroxyapatite particles.

## 4 Discussion

Generally, various hydroxyapatite composites have been prepared by traditional techniques by mixing raw materials components together and specimens were then produced by moulding into desired shape using heat or chemical reaction for example compression moulding, injection moulding or casting. In this study, bioactive composites of

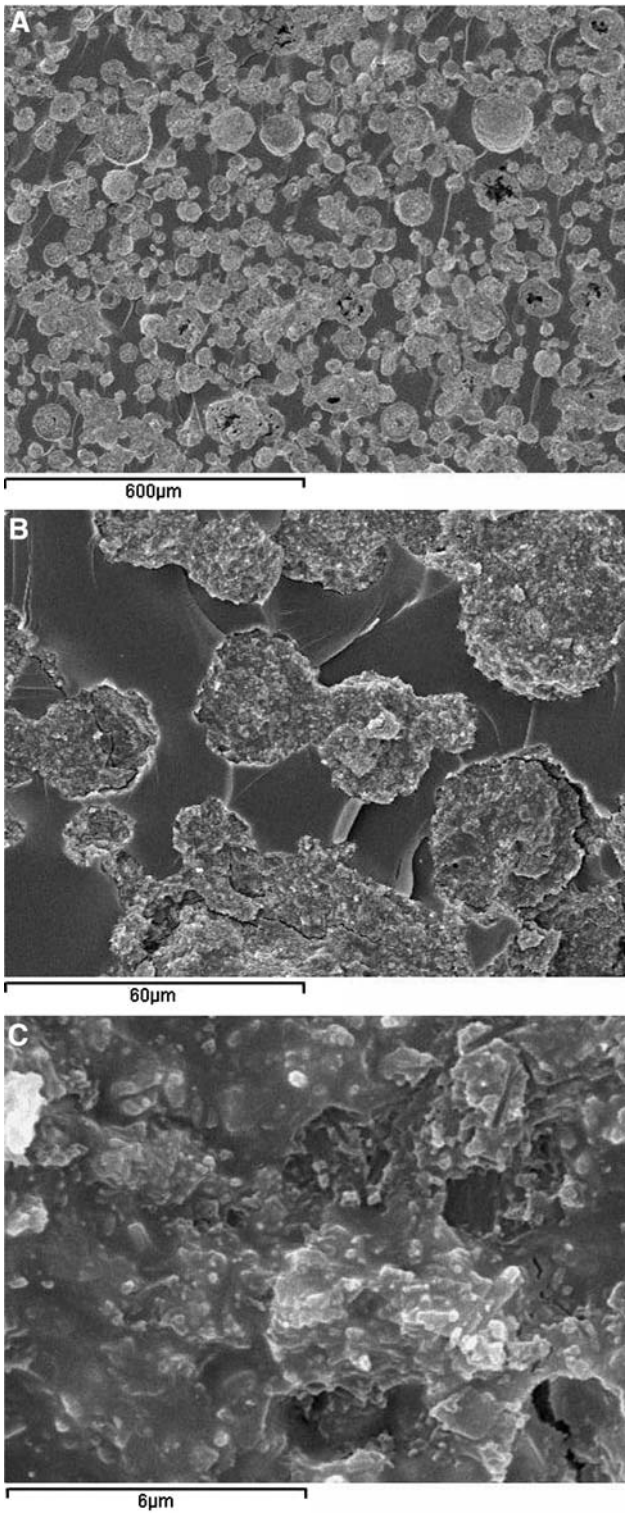


**Fig. 6** Fracture surface of HA-bisGMA-g 3DP composite after flexural testing

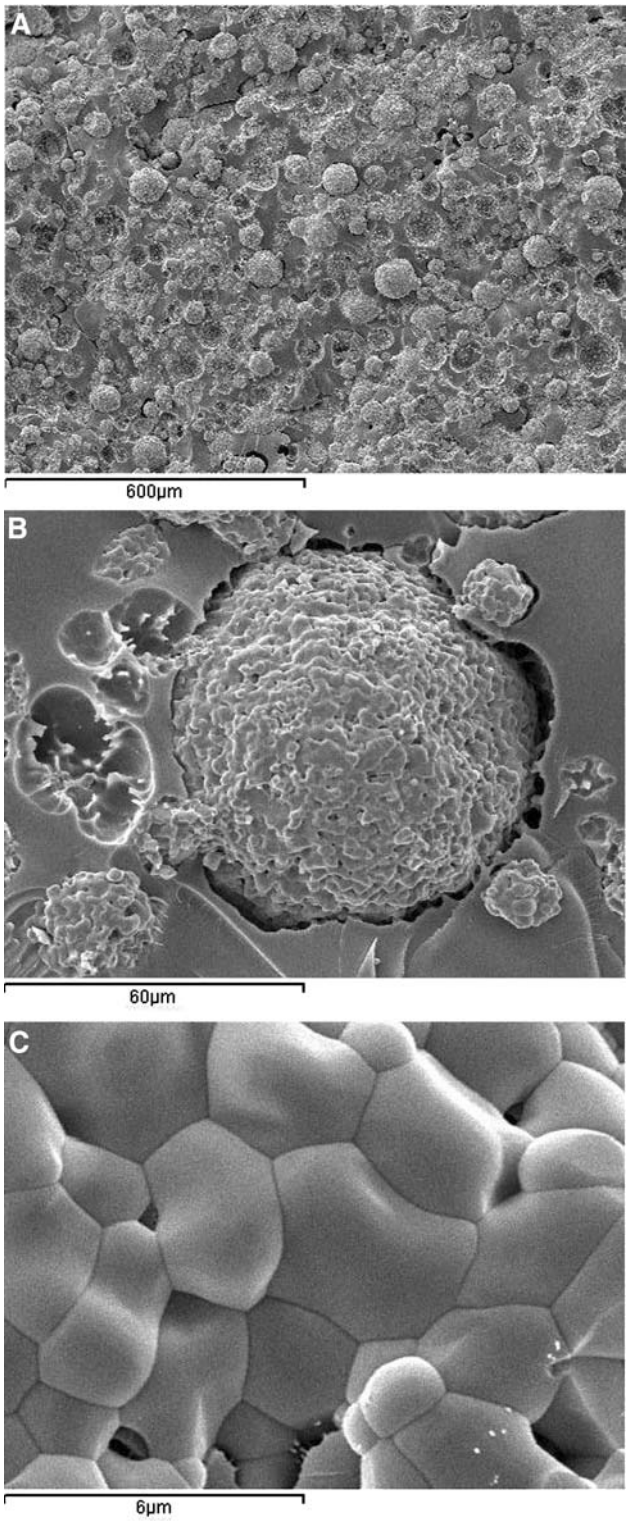


**Fig. 7** Fracture surface of HA-bisGMA-s 3DP composite after flexural testing

hydroxyapatite and bis-GMA based acrylate were prepared by a new technique namely 3DP which is one of freeform fabrication technologies. This new technique starts from firstly designing a required specimen in the computer and then exporting the image of designed specimen to the 3DP machine. Secondly, hydroxyapatite sample according to

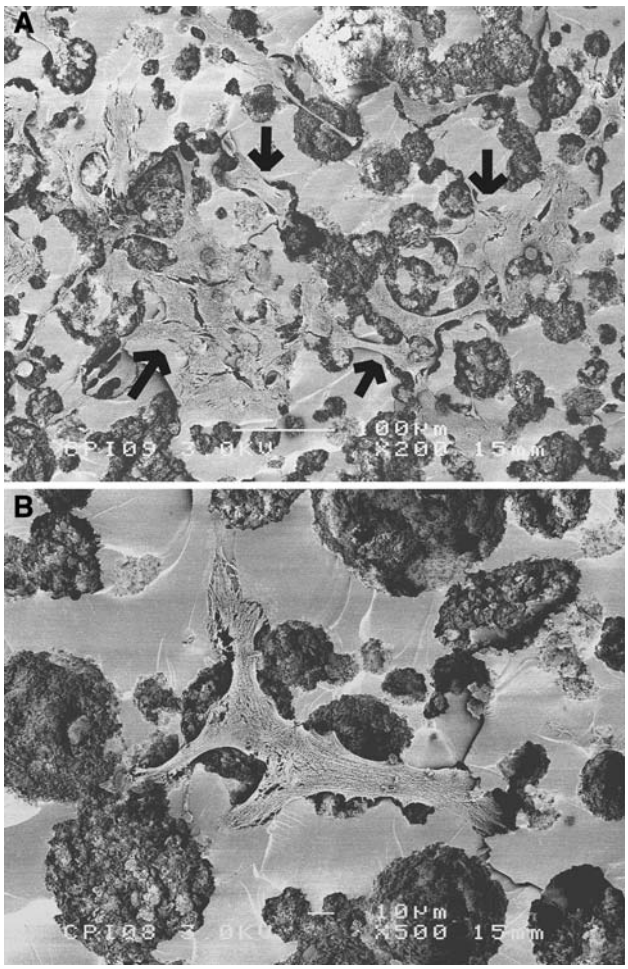


**Fig. 8** SEM micrograph of osteoblast cells on surface of HA-bisGMA-g 3DP composite after 6 days cultured

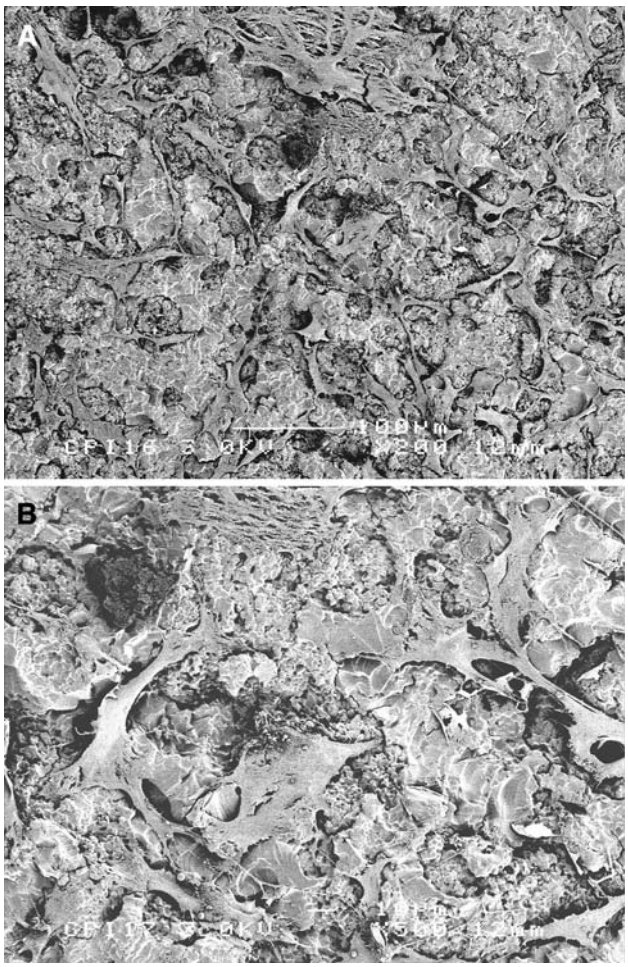


**Fig. 9** SEM micrograph of osteoblast cells on surface of HA-bisGMA-g 3DP composite after 6 days cultured

the designed shape was created directly by 3DP machine without using any moulds. Thirdly, bis-GMA based acrylate resin was then impregnated in the fabricated sample to produce bioactive composites. Two types of composites were studies. One was produced based on the as-fabricated green 3DP specimen, namely HA-bisGMA-g, and another one was generated from sintered 3DP specimen, namely HA-bisGMA-s.

The fabrication in this study employs the benefit of porous nature of 3DP specimen to produce composite. This porous structure is resulted from the characteristic of 3DP processing technique in that powders are lightly connected together by adhesive binder. Consequently, the 3DP parts always contain pores. It can be observed in Table 2 that the density of 3DP hydroxyapatite specimen is much less than theoretical density of hydroxyapatite (3,160 kg $m^{-3}$). After impregnating by bis-GMA based acrylate, the pores in the hydroxyapatite 3DP samples are filled up with the continuous resin matrix. Consequently, the densities of 3DP composites are significantly increased and are observed to be greater than those of 3DP hydroxyapatite and matrix resin. HA-bisGMA-s composite is slightly denser than HA-bisGMA-g since the original sintered 3DP hydroxyapatite specimen prior to composite impregnation is denser than the green 3DP hydroxyapatite. Sintering hydroxyapatite at high temperature caused the sample to shrink and decrease porosity. At the same time, the low density organic binder was also burnt out and removed from the sample. A comparison of experimental and calculated densities of composites using composite rule of mixture in couple with the volume fraction of hydroxyapatite in composites as determined by TGA and densities of each components is also shown in Table 2. It could be seen that the equation describes the dependency of density on the filler content well. Calculated values of both composites are within 8% of experimental values.

In general, mechanical properties of hydroxyapatite reinforced polymer composite could either increase or decrease with increasing hydroxyapatite content depending on the type of properties. While modulus and creep

resistance always increase with increasing amount of hydroxyapatite, the strength, impact toughness and strain at break normally decrease [1–5]. In this study, the dependency of modulus of composites on the filler volume fraction was observed to follow such trend. Modulus of HA-bisGMA-s is higher than HA-bisGMA-g since HA-bisGMA-s has higher content of hydroxyapatite than HA-bisGMA-g. The modulus data obtained experimentally were found to lie within the upper and lower bounds of the modulus predicted using the classic composite rule of mixture, Fig. 10. In contrast to modulus, flexural strength of HA-bisGMA-g is greater than HA-bisGMA-s composite. This could be explained on the basis of poor adhesion model of the particulated composite system which the strength is decreased with increasing filler content. In this system, as the particles debond from the matrix during loading due to poor interface adhesion, the load bearing area of the composite would decrease as only the matrix would carry the load. The stress experienced by the matrix would; thus, be increased and this would eventually fracture the supporting matrix. The strength is decreased with increasing filler content or decreasing in matrix content. Simple empirical models developed by Nicholais and Nakris [26] for a rigid matrix which assumes poor interfacial adhesion between matrix and fillers was plotted against the experimental strength data, Fig. 11. It was observed that the agreement between the experimental data and the model was very good which indicates the poor bonding between hydroxyapatite particles and bis-GMA based resin in both composites. In the case of strain at break, it was observed to follow the similar trend as the strength. Flexural strain at break of HA-bisGMA-s which has higher hydroxyapatite contant is lower than HA-bisGMA-g composite. This is obviously due to the reduction of the matrix phase of composite with increasing filler content as the strain would come from the polymer if the filler is rigid. The interpretation of low interfacial bonding between hydroxyapatite and matrix resin as derived from mechanical property results is also confirmed by the fracture surfaces of both composites which show complete debonding of hydroxyapatite particles from bis-GMA matrix.

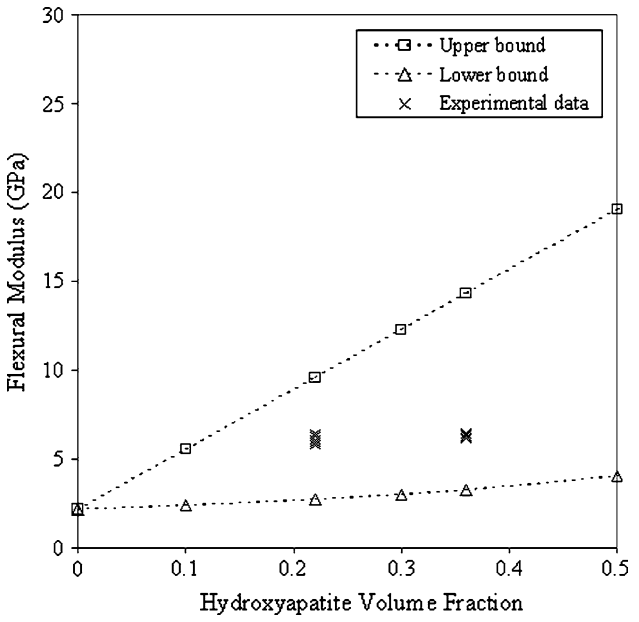


**Fig. 10** Variation of flexural modulus of hydroxyapatite/bis-GMA based composites with volume fraction of hydroxyapatite as compared with rule of mixture model (□ $E_c = E_f V_f + E_m V_m$; Δ $1/E_c = V_f/E_f + V_m/E_m$ where $E_c$, $E_f$ and $E_m$ are modulus of composite, filler and matrix, respectively, $V_f$ and $V_m$ are filler and matrix volume fraction respectively)

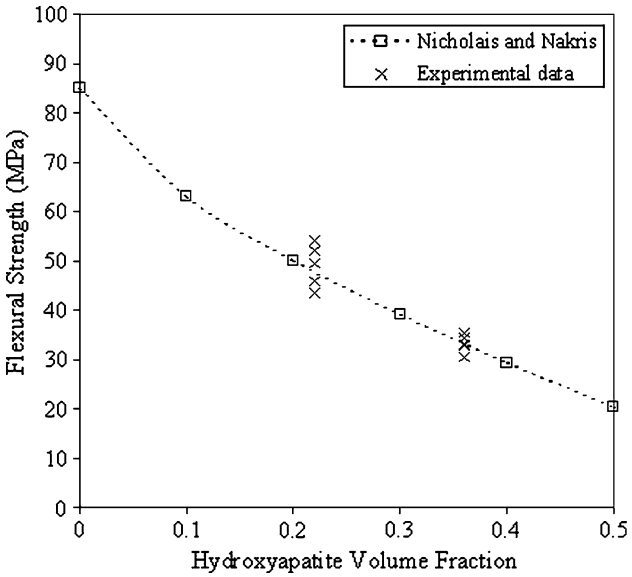


**Fig. 11** Variation of flexural strength of hydroxyapatite/bis-GMA based composites with volume fraction of hydroxyapatite as compared with Nicholais and Nakris model ($\sigma_c = \sigma_m [1–1.21\ V_f^{2/3}]$ where $\sigma_c$ and $\sigma_m$ are strength of composite and matrix, respectively, $V_f$ is filler volume fraction)

In comparison to previous hydroxyapatite/bis-GMA composites which were prepared by traditional moulding technique, the mechanical properties of both HA-bisGMA-g and HA-bisGMA-s 3DP composites lie in a range of reported values which are about 25–95 MPa for flexural strength and 4–11 GPa for modulus depending on the compositions, modification and types of materials used [10–13]. From the application point of view, the mechanical properties of 3DP composites are also in the range of trabecular bone and some synthetic materials that are normally employed as an implant for reconstructive surgery for example porous polyethylene, polymethyl methacrylate bone cement and silicone [27–29] and even closed to the lower range of mechanical properties of compact bone (modulus ~7–30 GPa and strength ~50–150 MPa) [30, 31].

In the case of bioactivity, the achieved hydroxyapatite volume fraction in the 3DP composites as demonstrated in this study which are 0.22 and 0.36 are supposed to be sufficient for composite to yield acceptable biocompatibility. It was shown previously that bioactivity of composites increases with increasing hydroxyapatite [1, 6–9]. Hydroxyapatite provides a favourable site for cell attachment, with cell processes frequently observed anchoring to the HA particles [6, 7]. This attachment has critical implications with respect to growth, proliferation and differentiation. Once the cells have attached, they are able to modify their environment by producing various growth factors and cytokinins, and the synthesis of extra cellular matrix components. It was also reported that volume fractions of hydroxyapatite in hydroxyapatite/polyethylene composite greater than 0.20 exhibited no adverse effect with adhearnce with tissue after implanted in lateral condyle of New Zealand White rabbits [8]. However, 0.40 volume fraction appeared to produce higher organised collagenous matrix, and higher levels of ALP activity than the 0.20 volume fraction [9]. Therefore, these three dimensionally printed hydroxyapatite/bis-GMA based composites should show no adverse effect and should be able to be used as bioactive bone replacement implant. The advantage of this fabrication technique compared to others is that the implants can be customized and the there is virtually no limitation in the complexity of the shape that can be designed and fabricated.

## 5 Conclusion

Two types of bioactive hydroxyapatite/bis-GMA based composites were fabricated successfully using 3DP technique in couple with resin impregnation. The hydroxyapatite volume contents in both composites were found to be 0.22 and 0.36 which are typical levels that could show bioactivity of the composites without compromising the mechanical properties. Composite produced from as-fabricated 3DP hydroxyapatite shows higher strength and strain at break than composite produced from high temperature sintered sample. However, the bioactivity of composite produced from sintered sample should be higher due to the greater amount of hydroxyapatite in the composite. Poor interfacial bonding between hydroxyapatite and matrix resin was observed in both composites. The improvement of the interfacial bonding should be studied in the future to increase the mechanical properties of the composites.

**Acknowledgement** National Metal and Materials Technology Center, National Science and Technology Development Agency is grateful for the financial support.

## References

1. W. Bonfield, Ann. NY Acad. Sci. **523**, 173 (1988)
2. J. Suwanprateeb, K.E. Tanner, S. Turner, W. Bonfield, J. Mater. Sci.: Mater. Med. **6**, 804 (1995)
3. J. Suwanprateeb, K.E. Tanner, S. Turner, W. Bonfield, J. Mater. Sci.: Mater. Med. **8**, 469 (1997)
4. J. Suwanprateeb, K.E. Tanner, S. Turner, W. Bonfield, J. Biomed. Mater. Res. **39**(1), 16 (1998)
5. Y. Zhang, K.E. Tanner, J. Mater. Sci.: Mater. Med. **14**, 63 (2003)
6. J. Huang, L. Di Silvio, M. Wang, K.E. Tanner, W. Bonfield, J. Mater. Sci.: Mater. Med. **8**(12), 775 (1997)
7. M.J. Dalby, L. Di Silvio, E.J. Harper, W. Bonfield, J. Mater. Sci.: Mater. Med. **10**, 793 (1999)
8. W. Bonfield, J.C. Behiri, C. Doyle, J. Bowman, J. Abram, in "Biomaterials and Biomechanics", edited by P. Ducheyne, G.V. Perre, A.A.E. Aubert (Elsevier Science Publishers, Amsterdam, 1983) p. 421
9. L. Di Silvio, M.J. Dalby, W. Bonfield, Biomaterials **23**, 101 (2002)
10. C. Santos, Z.B. Luklinska, R.L. Clarke, K.W.M. Davy, J. Mater. Sci.: Mater. Med. **12**, 565 (2001)
11. R.W. Arcis, A. Lopez-Macipe, M. Toledano, E. Osorio, R. Rodriguez-Clemente, J. Murtra, M.A. Fanovich, C.D. Pascual, Dent. Mater. **18**, 49 (2002)
12. S. Deb, L. Aiyathurai, J.A. Roether, Z.B. Luklinska, Biomaterials **26**, 3713 (2005)
13. W.R. Walsh, M.J. Svehla, J. Russell, M. Saito, T. Nakashima, R.M. Gillies, W. Bruce, R. Hori, Biomaterials **25**, 4929 (2004)
14. D.T. Pham, R.S. Gault, Int. J. Mach. Tool Manuf. **38**, 1257 (1998)
15. K. Dellef, C.K. Chua, Z.H. Du, Comput. Ind. **39**, 3 (1999)
16. W. Guangchun, L. Huiping, G. Yanjin, Z. Guoqun, Rapid Prototyping J. **10**(3), 200 (2004)
17. P. Potamianos, A.A. Amis, A.J. Forester, M. Mcgurk, M. Bircher, Proc. Instn Mech Engrs. **212**, 383 (1998)
18. H. Jee, E. Sachs, Rapid Prototyping J. **6**(1), 50 (2000)
19. B. Sanghera, S. Naique, Y. Papaharilaou, A. Ames, Rapid Prototyping J. **7**(5), 275 (2001)
20. F.E. Wiria, K.F. Leong, C.K. Chua, Y. Liu, Acta Biomater. **3**(1), 1 (2007)
21. M.N. Cooke, J.P. Fisher, D. Dean, C. Rimnac, A.G. Mikos, J. Biomed. Mater. Res. B Appl. Biomater. **64B**, 65 (2002)
22. I. Zein, D.W. Hutmacher, K.C. Tan, S.H. Teoh, Biomaterials **23**, 1169 (2002)
23. K.H. Tan, C.K. Chua, K.F. Leong, C.M. Cheah, P. Cheang, M.S. Bakar Abu, S.W. Cha, Biomaterials **24**, 3115 (2003)
24. J.T. Rimell, P.M. Marquis, J. Biomed. Mater. Res. B Appl. Biomater. **53**, 414 (2000)
25. R. Chumnanklang, T. Panyathammaporn, K. Sitthiseripratip, J. Suwanprateeb, Mater. Sci. Eng. C **27**, 914 (2007)
26. L. Nicholais, M. Nakris, Polym. Eng. Sci. **11**, 194 (1971)
27. J. Black, G. Hastings, in "Handbook of Biomaterial Properties" (Chapman & Hall, London, 1998)
28. ASTM F755-99e1 Standard Specification for Selection of Porous Polyethylene for Use in Surgical Implants. ASTM International
29. P. Van Landuyt, B. Peter, L. Beluze, J. Lemaitre, Bone **25**, 95s (1999)
30. I. Oh, N. Nomura, N. Masahashi, S. Hanada, Scr. Mater. **49**(12), 1197 (2003)
31. M. Milosevski, J. Bossert, D. Milosevski, N. Gruevska, Ceram. Int. **25**(8), 693 (1999)